Acta Crystallographica Section C
Crystal Structure Communications
ISSN 0108-2701

Bis(2,6-diamino-1*H*-purin-3-ium) di-μ-croconato-$\kappa^3O,O':O'';\kappa^3O:O',O''$-bis[tetraaqua(croconato-κ^2O,O')-neodymium(III)]

Ana María Atria,[a] Mauricio Morel,[b] Maria Teresa Garland[c]* and Ricardo Baggio[d]*

[a]Facultad de Ciencias Químicas y Farmacéuticas, Universidad de Chile, Casilla 233, Santiago, Chile, [b]Departamento de Física, Facultad de Ciencias Físicas y Matemáticas, Universidad de Chile, Santiago de Chile, Chile, [c]Departamento de Física, Facultad de Ciencias Físicas y Matemáticas and CIMAT, Universidad de Chile, Santiago de Chile, Chile, and [d]Departamento de Física, Centro Atómico Constituyentes, Comisión Nacional de Energía Atómica, Buenos Aires, Argentina
Correspondence e-mail: mtgarlan@dfi.uchile.cl, baggio.ricardo@gmail.com

Received 9 December 2010
Accepted 16 December 2010
Online 18 December 2010

The structure of the ionic title compound, $(C_5H_7N_6)_2[Nd_2(C_5O_5)_4(H_2O)_8]$, consists of anionic dimers built around an inversion centre and is made up of an Nd^{III} cation, two croconate (croco) dianions and four water molecules (plus their inversion images), with two noncoordinated symmetry-related 2,6-diamino-1*H*-purin-3-ium ($Hdap^+$) cations providing charge balance. Each Nd^{III} atom is bound to nine O atoms from four water and three croco units. The coordination polyhedron has the form of a rather regular monocapped square antiprism. The croconate anions are regular and the $Hdap^+$ cation presents a unique, thus far unreported, protonation state. The abundance of hydrogen-bonding donors and acceptors gives rise to a complex packing scheme consisting of dimers interlinked along the three crystallographic directions and defining anionic 'cages' where the unbound $Hdap^+$ cations lodge, linking to the mainframe *via* $(N-H)_{Hdap}\cdots O_{water/croco}$ and $(O-H)_{water}\cdots N_{Hdap}$ interactions.

Comment

2,6-Diaminopurine (dap) is a highly interactive entity that, because of its many active sites, can take part in complex hydrogen-bonding interaction networks, either as a donor or acceptor. In spite of these capabilities, few structures including the molecule are known so far. We have recently reported (Atria *et al.*, 2010) two structures in which the molecule acts as a free base [2,6-diamino-9*H*-purine monohydrate, (II*a*)] and as a cation [bis(2,6-diamino-9*H*-purin-1-ium) 2-(2-carboxylatophenyl)acetate heptahydrate, (II*b*)], and in both a complicated hydrogen-bonding scheme builds up as a result of the intermolecular interactions.

Croconate (croco), the dianion of 4,5-dihydroxycyclopent-4-ene-1,2,3-trione, $C_5O_5^{2-}$, is a member of the cyclic oxocarbon family of general formula C_nO_n (n = 3, deltate; n = 4, squarate; n = 5, croconate; and n = 6, rhodizonate). It can act

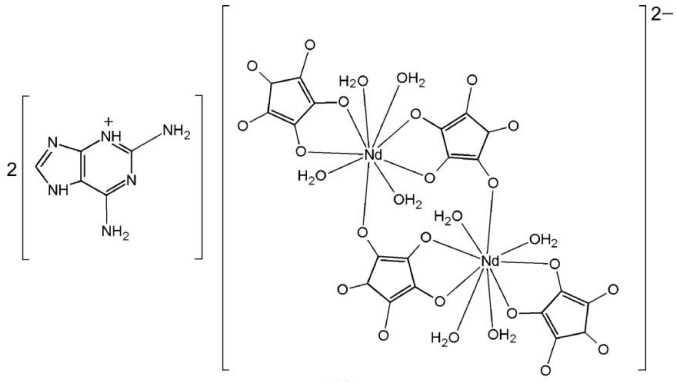

(I)

as a versatile polydentate ligand owing to its five different coordination sites, thus enabling it to bind to metal ions *via* an

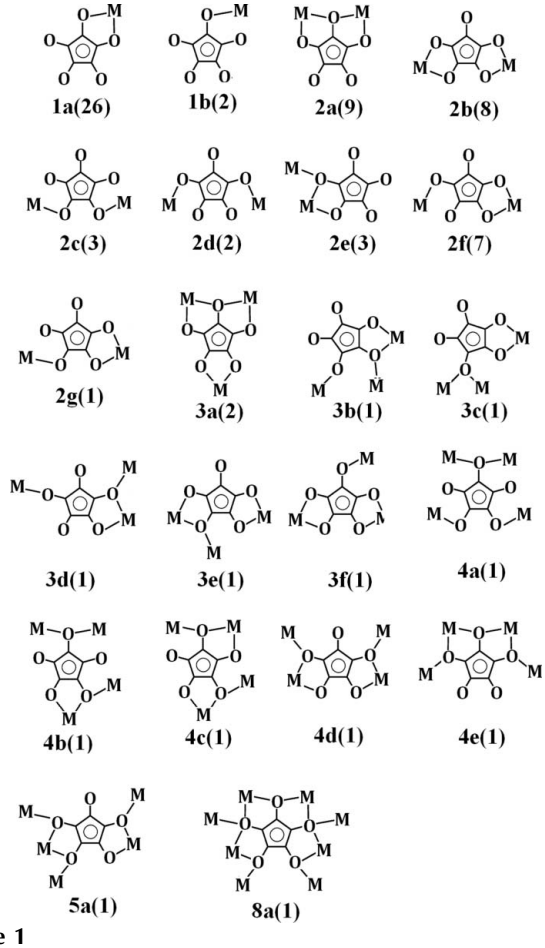

Figure 1
The binding modes shown by the croconate ligand. Explanation of the [$\mu\kappa$**(n)**] symbol: μ is the number of metal atoms bridged by the ligand, κ is the sequential label within the μ group and **n** is the number of entries found in the CSD for the $\mu\kappa$ mode.

 doi:10.1107/S0108270110052893

impressive number of different coordination modes, many of them only recently reported. Fig. 1 presents an updated survey of the 22 different modes adopted by croconate in complexes [Cambridge Structural Database (CSD), Version 5.31; Allen, 2002], sorted in ascending order of coordination number and covering the range 1 to 5 plus an amazing outlier with $\mu = 8$.

In pursuit of our current interest in lanthanide metal–organic frameworks (MOFs) with profuse hydrogen-bonding interactions, the inclusion of both dap and croco was an appealing prospect both from the coordination as well as the hydrogen-bonding point of view. Herein we present the first successful results in this series, with Nd as the lanthanide. The Nd–croconate complex obtained, *viz.* $2Hdap^{+}\cdot\{[Nd^{III}(croco)_2(H_2O)_4]_2\}^{2-}$, (I), even if not a polymer as expected, presents an attractive dimeric structure with tight noncovalent interlinkage, leading to a 'nested' hydrogen-bonding structure.

Dinuclear units of (I) are built up around an inversion centre (Fig. 2), the independent part consisting of a Nd^{III} centre, two croconate anions and four water molecules. The two negative charges of the resulting dimer are balanced by two noncoordinated symmetry-related $Hdap^{+}$ cations. Each $Hdap^{+}$ is coordinated by nine O atoms in total (Table 1), four of them water molecules [O1*W*→O4*W*; Nd—O_{water} range = 2.439 (2)–2.555 (2) Å], the remaining five are provided by three croco groups [O12, O22, O11, O21 and O31^{i}; symmetry code: (i) $-x+2, -y+2, -z+1$; Nd—O_{croco} range = 2.455 (2)–2.570 (2) Å]. The coordination polyhedron has the form of a rather regular monocapped square antiprism (Fig. 2, inset), with O1*W* in the capping position and (O12, O22, O3*W* and O31^{i}) and (O11, O21, O2*W* and O4*W*) defining the upper/lower bases, respectively. One of the croco anions (trailing label 2, croco2) acts in a simple κ^2O,O'-chelating fashion though O12 and O22, while the remaining one (trailing label 1, croco1), in addition to chelation *via* O11 and O21, also involves a third oxygen (O31), displaying a final $\mu_2,\kappa^3O,O':O''$-coordination mode. This results in the formation of large (Nd–O–C–C–O)$_2$ centrosymmetric bridging rings, linking individual $Nd(croco)_2(H_2O)_4$ monomers into the dimeric structural units shown in Fig. 2.

The binding modes observed in (I) occur with different frequency in the literature. The first one is the most common (**1a** in Fig. 1) and 26 of the 66 entries in the CSD show this pattern, while the second is among the rarest (mode **2g** in Fig. 1) with only one appearance (Ghoshal *et al.*, 2005). In this latter structure, however, the bridging mode gives rise to an infinite corrugated two-dimensional assembly of copper coordination polyhedra instead of the isolated dimers found in (I).

The geometry of the croco ligands is regular and both moieties display symmetries close to D_{2h}. C—O bond lengths within each unit present maximum percentage differences of 1.6 and 2.9% for croco1 and croco2, respectively, which can be considered small when compared with other croco complexes in the literature [for example, Chen *et al.* (1990), with differences larger than 10.3% and symmetries closer to C_{2v}].

The $Hdap^{+}$ cation is planar, with a mean deviation of the atoms from the plane of 0.0193 (12) Å and a maximum departure from the least-squares plane (for atom C23) of 0.0431 (14) Å. Planarity extends to the two amino groups, which are coplanar with the rest of the molecule, and in this respect similar to the only other $Hdap^{+}$ unit so far reported [structure (II*b*); Atria *et al.*, 2010], but different from the neutral unprotonated ones presented either in the same paper or in Atria *et al.* (2009), in both of which one of the two amine N atoms is significantly pyramidal; this different degree of planarity in the NH_2 groups is not uncommon in diamino aromatic groups and might be due to the ability of the delocalized π-system of the ring to accommodate charge from one

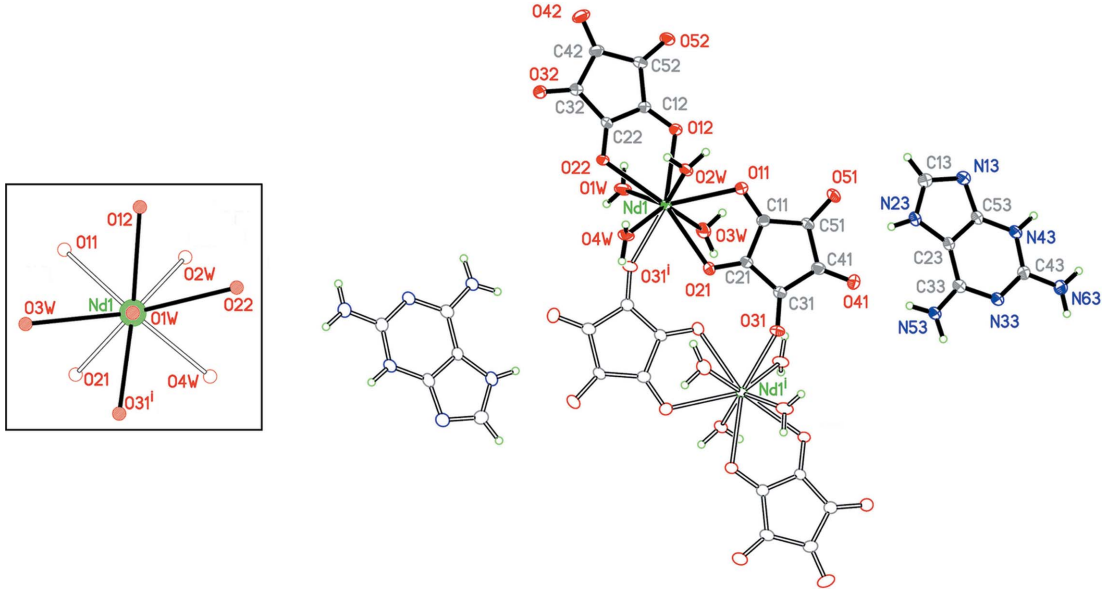

Figure 2
Displacement ellipsoid plot of the dimeric structure in (I) drawn at the 50% probability level, with independent (symmetry-related) atoms shown with heavy (hollow) bonds and filled (empty) ellipsoids. Inset: schematic of the coordination polyhedron. [Symmetry code: (i) $-x+2, -y+2, -z+1$.]

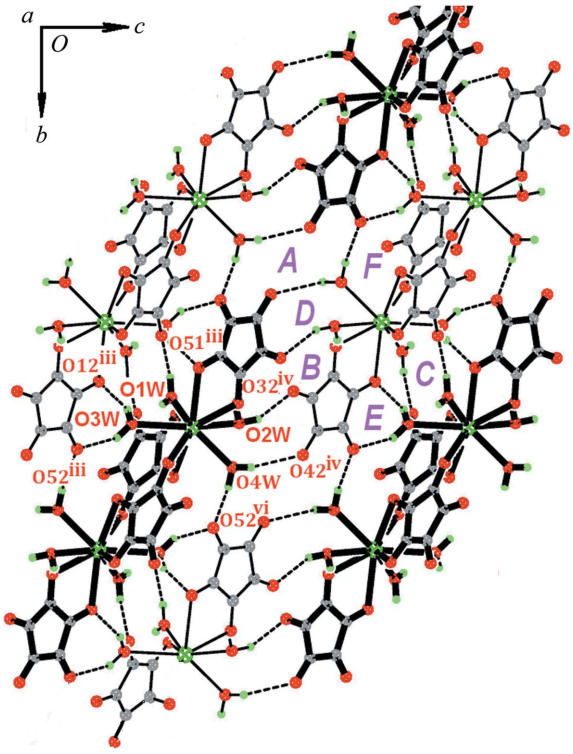

Figure 3
Packing plot of the two-dimensional structure parallel to the (100) plane and determined by interdimeric hydrogen bonds. Contiguous dimers are drawn in different shading for clarity. Hydrogen-bonding rings: '*A*' is $R_4^4(14)$; '*B*' is $R_2^2(14)$; '*C*' is $R_2^2(8)$; '*D*' is $R_2^2(9)$; '*E*' is $R_2^2(7)$; '*F*' is $R_1^1(11)$. [Symmetry codes: (ii) $x+1, y, z$; (iii) $-x+2, -y+1, -z+1$; (iv) $-x+2, -y+1, -z+2$; (v) $-x+1, -y+1, -z+1$; (vi) $x, y+1, z$.]

amino group, but not both, in the extended resonance structure (Linden, 2010).

Notwithstanding these analogies, there are also significant differences between the Hdap$^+$ ions in (I) and (II*b*). Protonation of diaminopurine takes place at different nitrogen sites, both at the imidazole [N2 in (I) and N1 in (II*b*)], as well as at the pyrimidine groups [N4 in (I) and N3 in (II*b*)]. This forces rearrangement of the charge distribution and the positioning of single/double bonds along the rings (see Scheme below).

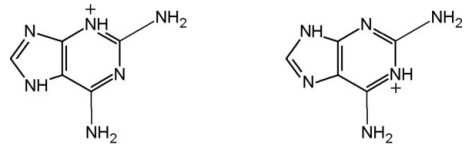

The outstanding hydrogen-bonding capability of Hdap$^+$, however, does not seem to be modified by the different H-atom disposition, as shown in Table 2. The table presents the 15 hydrogen bonds in the structure, which define a tight three-dimensional hydrogen-bonding network consisting of an (anionic) mesh of dimeric units (where all the water H atoms except H2*WB*, see below, are involved), giving rise to columnar 'cages' where the Hdap$^+$ cations reside.

The mesh can be imagined as built up in a two-step process: firstly, through six $(O-H)_{water}\cdots O_{croco}$ interactions (Table 2, entries 2–3 and 5–8) giving rise to six types of R_n^m rings

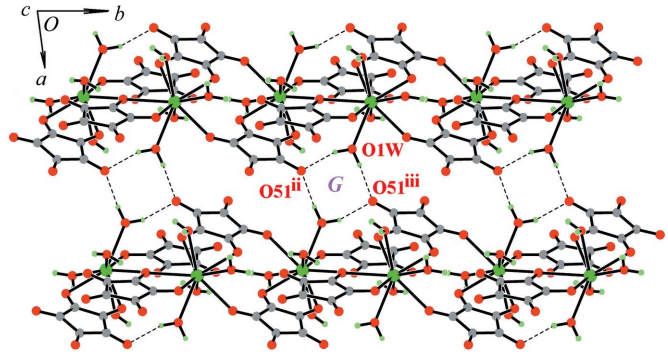

Figure 4
Projection down [001] showing the way in which the two-dimensional (100) dimeric structures shown in Fig. 3 interact. '*G*' represents the $R_4^2(8)$ hydrogen-bonding ring. [Symmetry codes: (ii) $x+1, y, z$; (iii) $-x+2, -y+1, -z+1$.]

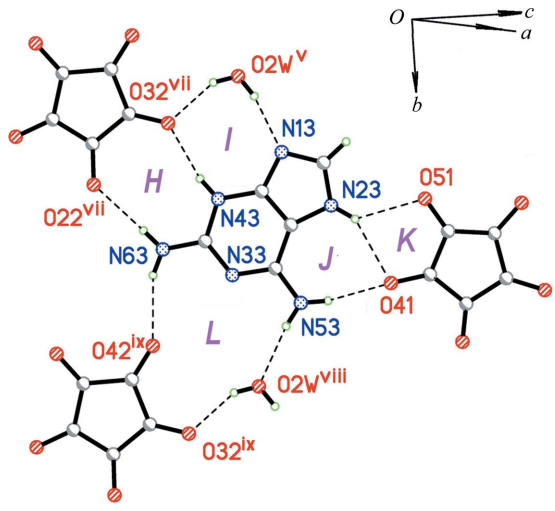

Figure 5
Interaction scheme of a single Hdap$^+$ cation, generating planar arrays parallel to $(\bar{1}01)$. Hydrogen-bonding rings: '*H*' is $R_2^2(9)$; '*I*' is $R_3^2(8)$; '*J*' is $R_2^1(7)$; '*K*' is $R_1^2(5)$; '*L*' is $R_3^3(13)$. [Symmetry codes: (v) $-x+1, -y+1, -z+1$; (vi) $x, y+1, z$; (vii) $x-1, y, z-1$; (viii) $-x+1, -y+2, -z+1$; (ix) $x-1, y+1, z-1$.]

(Bernstein *et al.*, 1995) and defining broad two-dimensional structures parallel to (100) (Fig. 3); secondly, through the connection of these 'planes' along [100] *via* the hydrogen bonds involving O1*W* (Table 2, entries 1–2, and Fig. 4).

These interconnections define the columnar 'cages' centred at $x \sim 0.5$, $z \sim 0.0$ and evolving along [010]; O2*W* is the only water molecule not entirely devoted to 'mesh building', but it acts instead as a bridge joining both ion types. Thus, the Hdap$^+$ counter-ions in the 'cages' link to the mainframe through this latter $(O-H)_{water}\cdots N_{Hdap}$ bond (Table 2, entry 4), and *via* one $(N-H)_{Hdap}\cdots O_{water}$ (Table 2, entry 13) and six $(N-H)_{Hdap}\cdots O_{croco}$ interactions (Table 2, entries 9–12 and 14–15). This gives rise to a large number of hydrogen-bonding rings, displayed in Fig. 5, where the nearest-neighbour environment of one such Hdap$^+$ cation is shown. This is a strikingly planar two-dimensional substructure where all aromatic rings (both the free Hdaps as well as the coordinated croco ligands) lie almost parallel to each other, with a mean deviation of 0.196 (8) Å from their least-squares plane, parallel to $(\bar{1}01)$.

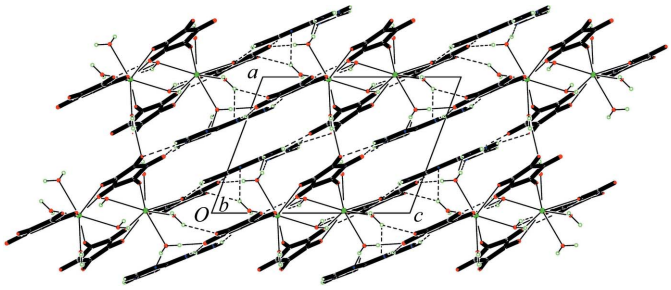

Figure 6
Packing plot along [010], showing in projection (heavy lining) the planar structures shown in Fig. 5.

These planar arrays are a direct consequence of the extreme directionality of the hydrogen bonds connecting the intervening aromatic units. Similarly, planar dispositions have already been described in a number of structures containing dap or Hdap derivatives, either crystallizing alone [for example, (II*a*) in Atria *et al.* (2010)] or with aromatic partners [for example, Sakore *et al.* (1969) and (II*b*) in Atria *et al.* (2010)]. In all these cases, these planes are arranged in pairs, parallel to each other at a graphitic distance from one another, usually the result of a number of π–π interactions connecting planes. In the present case, however, even if a similar 'multilayer' structure of such planes exists (Fig. 6), the possibility of optimizing stacking interactions appears precluded by coordination of the croco ligands, which anchors them relative to the cation sites in detriment of an optimal stacking geometry. This was confirmed with the help of the program *PLATON* (Spek, 2009), which did not indicate any relevant π–π contacts between layers.

The most appealing aspects of compound (I), as in related dap/Hdap structures that we have studied so far (Atria *et al.*, 2009, 2010), reside in the rich supramolecular structure arising from the ensemble of simple but highly interacting molecular units. We are currently working towards obtaining new members of this lanthanide–(dap/Hdap) family.

Experimental

An ethanolic solution of croconic acid (0.050 g, 0.035 mmol) and 2,6-diaminopurine (0.070 g, 0.47 mmol) was added to an aqueous solution (400 ml) of neodymium nitrate (0.1539 g, 0.35 mmol), previously heated to about 343–353 K for 10 min under a nitrogen atmosphere. The reaction mixture was refluxed for 24 h, cooled to room temperature and filtered. Crystals adequate for X-ray diffraction analysis were obtained within a few days by slow evaporation of the solution. The whole process was carried out in the dark.

Crystal data

$(C_5H_7N_6)_2[Nd_2(C_5O_5)_4(H_2O)_8]$
M_r = 1295.14
Triclinic, $P\overline{1}$
a = 9.0999 (5) Å
b = 9.5912 (5) Å
c = 12.3272 (7) Å
α = 89.133 (3)°
β = 69.418 (2)°
γ = 82.740 (3)°
V = 998.66 (9) Å^3
Z = 1
Mo $K\alpha$ radiation
μ = 2.70 mm^{-1}
T = 150 K
0.24 × 0.19 × 0.16 mm

Data collection

Bruker SMART CCD area-detector diffractometer
Absorption correction: multi-scan (*SADABS* in *SAINT-NT*; Bruker, 2002)
T_{min} = 0.55, T_{max} = 0.65
16172 measured reflections
4379 independent reflections
4089 reflections with $I > 2\sigma(I)$
R_{int} = 0.027

Refinement

$R[F^2 > 2\sigma(F^2)]$ = 0.031
$wR(F^2)$ = 0.082
S = 1.11
4379 reflections
371 parameters
14 restraints
H atoms treated by a mixture of independent and constrained refinement
$\Delta\rho_{max}$ = 3.30 e Å^{-3}
$\Delta\rho_{min}$ = −0.87 e Å^{-3}

Table 1
Selected bond lengths (Å).

Nd1—O4*W*	2.439 (2)	Nd1—O3*W*	2.540 (3)
Nd1—O31^{i}	2.455 (2)	Nd1—O2*W*	2.555 (2)
Nd1—O1*W*	2.472 (3)	Nd1—O22	2.560 (2)
Nd1—O11	2.501 (2)	Nd1—O21	2.570 (2)
Nd1—O12	2.526 (2)		

Symmetry code: (i) $-x+2, -y+2, -z+1$.

Table 2
Hydrogen-bond geometry (Å, °).

D—H···A	D—H	H···A	D···A	D—H···A
O1*W*—H1*WA*···O51^{ii}	0.83 (2)	2.03 (3)	2.798 (4)	154 (4)
O1*W*—H1*WB*···O51^{iii}	0.84 (2)	1.91 (2)	2.704 (3)	158 (4)
O2*W*—H2*WA*···O32^{iv}	0.83 (2)	1.99 (3)	2.761 (3)	154 (4)
O2*W*—H2*WB*···N13^{v}	0.83 (2)	2.01 (2)	2.833 (4)	168 (4)
O3*W*—H3*WA*···O52^{iii}	0.82 (2)	2.52 (4)	3.028 (3)	121 (4)
O3*W*—H3*WB*···O12^{iii}	0.83 (2)	1.99 (2)	2.820 (3)	174 (4)
O4*W*—H4*WA*···O52^{vi}	0.84 (2)	1.84 (2)	2.673 (3)	170 (4)
O4*W*—H4*WB*···O42^{iv}	0.83 (2)	2.31 (3)	2.993 (4)	140 (4)
N23—H23···O51	0.86 (2)	2.27 (3)	2.931 (4)	134 (4)
N23—H23···O41	0.86 (2)	2.27 (3)	3.025 (4)	147 (4)
N43—H43···O32^{vii}	0.85 (2)	1.99 (2)	2.807 (4)	163 (4)
N53—H53*A*···O41	0.84 (2)	2.02 (2)	2.847 (4)	169 (4)
N53—H53*B*···O2*W*^{viii}	0.86 (2)	2.28 (3)	3.095 (4)	159 (4)
N63—H63*A*···O42^{ix}	0.86 (2)	2.29 (3)	3.062 (4)	149 (5)
N63—H63*B*···O22^{vii}	0.84 (2)	2.10 (2)	2.930 (4)	172 (4)

Symmetry codes: (ii) $x+1, y, z$; (iii) $-x+2, -y+1, -z+1$; (iv) $-x+2, -y+1, -z+2$; (v) $-x+1, -y+1, -z+1$; (vi) $x, y+1, z$; (vii) $x-1, y, z-1$; (viii) $-x+1, -y+2, -z+1$; (ix) $x-1, y+1, z-1$.

The two largest residual electron-density peaks (*ca* 3.30 e Å^{-3}) lie opposite each other at 0.85 Å from atom Nd1. All H atoms were clearly visible in a difference Fourier maps, but were treated differently in the refinement. H atoms attached to C atoms were repositioned at their calculated locations and allowed to ride (C—H = 0.95 Å). Those attached to O and N atoms were further refined with a restrained O/N—H distance of 0.85 (2) Å (an s.u. of 0.01 Å was used to restrain the O—H distances in waters O3*W* and O4*W*). In all cases, U_{iso}(H) values were taken as 1.2U_{eq}(host). There is an artifact regarding refinement which is not unique to the present structure but has already been observed in other complexes we recently reported (Perec & Baggio, 2010). Although there is clear synthetic and analytical evidence for the composition of the title compound (see

Experimental), significantly lower *R* indices can be obtained when the structure is refined with a different metallic species (in the present case, for instance, La instead of Nd). However, despite many indicators favouring the substituting cation (lower *R* factors, smaller residual electron-density peaks, *etc.*), the Hirshfeld tests implemented in *PLATON checkCIF* generate a high number of alerts for the La refinement but none for the Nd refinement, thus indicating an incorrect assignment of atom type in the former case. We have no simple explanation for this paradox.

Data collection: *SMART* (Bruker, 2001); cell refinement: *SAINT-NT* (Bruker, 2002); data reduction: *SAINT-NT*; program(s) used to solve structure: *SHELXS97* (Sheldrick, 2008); program(s) used to refine structure: *SHELXL97* (Sheldrick, 2008); molecular graphics: *SHELXTL* (Sheldrick, 2008); software used to prepare material for publication: *SHELXTL* and *PLATON* (Spek, 2009).

We acknowledge the Spanish Research Council (CSIC) for providing us with a free-of-charge licence to the CSD system (Allen, 2002). We are also grateful for funding by Fondecyt (project Nos. 1070298 and 7090064).

Supplementary data for this paper are available from the IUCr electronic archives (Reference: MX3042). Services for accessing these data are described at the back of the journal.

References

Allen, F. H. (2002). *Acta Cryst.* B**58**, 380–388.
Atria, A. M., Astete, A., Garland, M. T. & Baggio, R. (2009). *Acta Cryst.* C**65**, m411–m414.
Atria, A. M., Garland, M. T. & Baggio, R. (2010). *Acta Cryst.* C**66**, o547–o552.
Bernstein, J., Davis, R. E., Shimoni, L. & Chang, N.-L. (1995). *Angew. Chem. Int. Ed. Engl.* **34**, 1555–1573.
Bruker (2001). *SMART*. Version 5-624. Bruker AXS Inc., Madison, Wisconsin, USA.
Bruker (2002). *SAINT-NT*. Version 6-22a (including *SADABS*). Bruker AXS Inc., Madison, Wisconsin, USA.
Chen, Q., Liu, S. & Zubieta, J. (1990). *Inorg. Chim. Acta*, **175**, 241–245.
Ghoshal, D., Ghosh, A. K., Ribas, J., Mostafa, G. & Chaudhuri, N. R. (2005). *CrystEngComm*, **7**, 616–620.
Linden, A. (2010). Personal communication.
Perec, M. & Baggio, R. (2010). *Acta Cryst.* C**66**, m339–m342.
Sakore, T. D., Sobell, H. M., Mazza, F. & Kartha, G. (1969). *J. Mol. Biol.* **43**, 385–406.
Sheldrick, G. M. (2008). *Acta Cryst.* A**64**, 112–122.
Spek, A. L. (2009). *Acta Cryst.* D**65**, 148–155.